Synchronous Parallel Ultrasound Induces Long-Term Extracellular Matrix Remodeling of Human Skin

Jean Carruthers, MD,* Virginia Benitez Roig, MD,†‡§ David H. McDaniel, MD, FAAD,‖¶ Brooke Jackson, MD, FAAD,** Oleg Bedich, MSc,†† Ruthie Amir, MD,†† and Shimon Eckhouse, PhD‡‡

BACKGROUND Energy-based interventions improve signs of skin aging by inducing controlled thermal injury and activating regenerative wound healing pathways.

OBJECTIVE This study investigates the underlying mechanism of acute and long-term extracellular matrix (ECM) remodeling induced by Synchronous Parallel Ultrasound technology leading to skin regeneration.

METHODS/MATERIALS An in vivo porcine model was used to investigate the acute thermal injury. In vivo human skin biopsies were obtained from subjects at baseline and at 1, 4, 7, and 10 months post-treatment. Histological evaluation was performed using Hematoxylin and Eosin, Masson's Trichome, Verhoeff–Van Gieson, Unna Taenzer, and Alcian Blue stains to assess changes in ECM protein expression.

RESULTS Thermal injury was restricted to the dermal layer. Histological analysis revealed a gradual increase in connective tissue collagen and elastin with unique reorganization and parallel realignment of the dermal fibers. Increased expression of glycosaminoglycans (GAGs) was also observed, indicating sustained fibroblast activity and matrix regeneration across all time points.

CONCLUSION These findings provide histological evidence of continuing and long-lasting dermal remodeling after Synchronous Parallel Ultrasound treatment, characterized by neocollagenesis, neoelastogenesis, and GAGs production. The study supports the efficacy of Synchronous Parallel Ultrasound in the long-term induction of skin regeneration.

The dermal extracellular matrix (ECM) is a complex and dynamic network that provides structural and mechanical support to the skin while mediating diverse biological processes that are crucial for supporting skin formation, function, and appearance.[1]

Within the dermis ECM, collagen fibers are organized around elastin-rich cores, forming a structurally integrated network. Collagen provides tissues with essential tensile strength, enabling resistance to plastic deformation and rupture, while elastin imparts extensibility and recoil, enabling the skin to withstand repetitive mechanical stress.[1–3] Normal levels of collagen and elastic fiber production, organization, and integration with other ECM constituents, such as proteoglycans and glycosaminoglycans (GAGs), are critical for preserving healthy skin structure, function, and youthful appearance.

The aging process is characterized by decreased levels of both collagen and elastin, driven by reduced biosynthetic activity of fibroblasts and by various extrinsic environmental factors.[4,5] These changes contribute to reduced skin elasticity and firmness, resulting in the formation of wrinkles and sagging skin, which are common aesthetic concerns.[3,6]

Cutaneous wound repair is a complex, dynamic, highly regulated process, involving multiple overlapping phases, including hemostasis and inflammation, characterized by the release of proinflammatory cytokines and growth factors (GFs), followed by the proliferation phase, during which activated fibroblasts synthesize collagen and elastin, and the remodeling phase, in which mesenchymal cells and ECM components reorganize into a mature, functionally integrated dermal matrix.[7,8]

Based on comprehensive understanding of the wound healing cascade and its key molecular players, several treatment interventions aiming at promoting skin regeneration have been developed. One such modality involves the application of controlled thermal injury to stimulate the production of dermal collagen, elastin, and hyaluronic acid (HA), achieved through optimal activation of the physiological wound healing response in the injured skin.

According to the Arrhenius equation, in vivo tissue injury and collagen denaturation are both time-dependent and

From the University of British Columbia, Vancouver, Canada; † Department of Laser Surgery and Aesthetic Medicine at Helicopteros Sanitarios Hospital, Marbella, Madrid, Spain; ‡ Department of Aesthetic Medicine and Cosmetic Surgery and Aesthetic and Functional Gynaecology and Cosmetic Genital Surgery for Women, Department of Dermato Aesthetic Pathology and Interventions at the University of Barcelona, Madrid, Spain; § Department of Dermato Aesthetic Pathology and Interventions at the University of Nebrija, Madrid, Spain; ‖ Institute of Aging Research and the Department of Biological Sciences, Old Dominion University, Hampton, Virginia; ¶ Skin of Color Research Institute, Hampton University, Hampton, Virginia; ** Skin Wellness Dermatology Associates, Durham, North Carolina; †† SofWave Medical, Israel; ‡‡ Alon Medtech Ventures and SofWave Medical, Israel.*

The authors have indicated no significant interest with commercial supporters.

Ruthie Amir is currently an employee of SofWave Medical in charge of clinical and regulatory.

Address correspondence and reprint requests to: Ruthie Amir, MD, SofWave Medical, 1 Ha-Otsma Street, 4th Floor, Yokneam Illit 2069200, Israel, e-mail: ruthie@Sofwave.com

Dermatol Surg 2025;51:S58–S64
http://dx.doi.org/10.1097/DSS.0000000000004793

temperature-dependent, with initial tissue damage beginning at approximately 43°C.[9] On exposure to elevated temperature, the triple helix collagen structure begins to denature and modify its 3D configuration by unfolding and shrinking. This process exposes the Arginylglycylaspartic acid (Arg-Gly-Asp) [RGD] ligands, which become accessible for interaction with compatible $\alpha\nu\beta_3$ integrins, leading to cell proliferation and increased cellular activity, resulting in the upregulation of collagen types I and III.[10–12] When considering the duration of thermal exposure, just a few seconds at 50 to 55°C can cause tissue damage and coagulation, while 65°C is the threshold temperature above which full collagen denaturation occurs.[13–15]

A new-generation ultrasound device has recently been introduced, using high-intensity, high-frequency, low-divergence, parallel ultrasound beams directed into the skin. The ultrasound transducers maintain effective mechanical contact with the skin and are actively cooled, ensuring that the upper layer of the skin remains at a low temperature preventing any thermal damage to the epidermis. The ultrasound frequency is carefully selected so that the energy is fully absorbed within the first 2 mm of the skin, which is a critical consideration for safe and effective treatment.[16] This configuration results in the formation of a localized heated zone at depths between 0.5 and 2 mm, specifically within the papillary and reticular dermis, while sparing both the epidermis and deeper anatomical structures. The use of an array of elongated rectangular transducers firing simultaneously produces a distinctive pattern of cylindrical, volumetric thermal injury zones, which are aligned parallel to both the skin surface and the longitudinal axis of each transducer.

Multiple studies have demonstrated the efficacy and safety of this approach for skin rejuvenation and lifting.[17–26] Here, the authors investigated the acute and long-term dermal ECM remodeling and regeneration using in vivo porcine model and human skin.

Materials and Methods

Synchronous Parallel Ultrasound Technology

The synchronous parallel ultrasound device (SUPERB, Sofwave, Yokne'am Illit, Israel) consists of 7 independently controlled, cooled piezoelectric transducers that emit ultrasonic energy simultaneously. For user-selectable energy levels of 3 to 5 Joules during the 5-second acoustic pulses, the fixed designed ultrasound frequency ensures that the energy is fully absorbed at optimal depths between 0.5 and 2 mm.

Histology–Porcine Experiments and Model Validation

A porcine model was used for the analysis of immediate post-treatment histology. During the development phase of SofWave technology, it was important to define the range of treatment parameters which are safe to use on human skin. Pig skin is the ideal model for research because of its high homology to human skin. Treatments were performed in vivo on the ventrolateral portion of a porcine model. Histological samples were formalin-fixed, stained using standard hematoxylin and eosin (H&E), and blindly assessed by a board-certified histopathologist. The width and depth of coagulated zones were measured using calibrated digital imaging equipment.

Histology–Human Skin

Skin biopsies were obtained before and after treatment from 11 healthy female patients across 3 independent investigational sites. Biopsies from the submentum are not easily visible and therefore were chosen for the study.

At 1 and 2 months post-treatment, submentum biopsies were collected from 4 subjects (ages: 50, 55, 60, and 63 years) treated at Dr. David McDaniel's clinic (McDaniel Institute of Aging Research, VA) and 5 subjects (ages: 63, 67, 70, 76, and 77 years) treated at Dr. Brooke Jackson's clinic (Skin Wellness Dermatology Associates, NC). Histological staining included H&E, Masson's Trichrome, and Verhoeff–Van Gieson.

Additional submentum biopsies were obtained from Pretreatment and 4, 7, and 10 months post-treatment from 3 female subjects (ages 40, 48, and 60 years) treated at Dr. Virginia Benitez's clinic (Laser Surgery & Aesthetic Medicine Department, Helicopter Sanitary Hospital, Marbella, Spain). Histological staining included H&E, Unna Taenzer, and Alcian Blue.

All studies were conducted in compliance with the Declaration of Helsinki. Signed informed consent and photograph consent were obtained from all subjects at each study site. Histopathological analysis was conducted by board-certified histopathologists.

Results

In Vivo Porcine Model

Thermal necrosis was predominantly restricted to the dermis (Figure 1). The epidermis remained intact, continuous, and with no abnormalities. In the superficial dermis, there were demarcated areas of coagulative necrosis, with swollen collagen and condensed nuclei, leading to disarray and structural disorder. The lesions were fractional and appeared flask-shaped, narrower at the surface, and wider at the base. No abnormal lesions were observed in the subcutaneous fat layer and the surrounding tissues. All

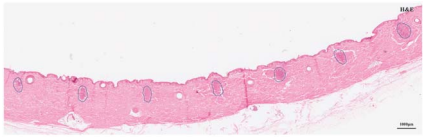

Figure 1. Representative post-treatment histological image of in vivo porcine skin. Tissue was stained with H&E. The blue demarcation outlines the zone of thermal coagulation induced by Synchronous Parallel Ultrasound technology at an energy setting of 4.6 joules. Scale bar: 1000 μm.

coagulative foci were within 2.0 mm depth from the epidermis. The tissue intervening 2 adjacent foci was normal.

The average lesion area was approximately 0.75 mm^2, with an average width of 1 mm and average depth of 1.2 mm. There was a significant correlation between different output energies and the thermal injury area size, the depth from the epidermis, and width.

In Vivo Human Biopsies

At 1-month post-treatment, a significant increase in dermal collagen density was observed, as indicated by darker and denser H&E staining (Figure 2). The increase was accompanied with a change in the whole morphology, from amorphous to highly organized, parallel alignment of collagen fibers. Mild epidermal thickening was noted, with preservation of epidermal integrity.

Masson's Trichrome staining at 1 month (Figure 3) demonstrated a significant increase in dermal collagen throughout the dermal layer. Additional fine fibrillar-like collagen fibers were observed in the upper dermal zone. The increased collagen density was accompanied by a more parallel arrangement of collagen fibers compared with the disorganization pattern at baseline. Epidermal thickness also seemed mildly increased.

Verhoeff–Van Gieson staining before and 1 month after treatment (Figure 4) demonstrated a significant increase in connective tissue elastin and collagen fibers, with distinct parallel alignment and structural order throughout the dermis. Elastin showed significant increases in the reticular dermis, evidenced by thicker bundles, while collagen was most increased in the mid and papillary dermis.

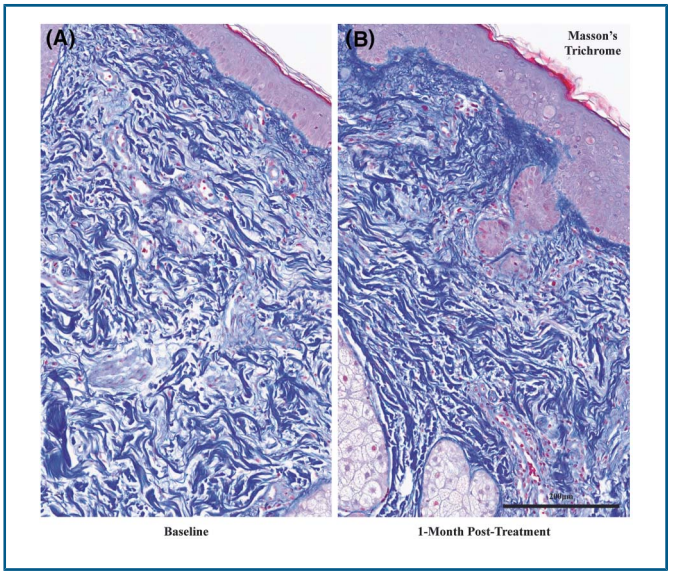

Figure 3. Masson's Trichrome staining at 1-month post-treatment. Representative submental skin biopsies from a 50-year-old woman with Fitzpatrick skin type I. Pretreatment (A) and 1-month post-treatment (B) images show the epidermal and dermal layers. Collagen fibers within the dermis appear blue. Scale bar: 200 μm.

At 2 months post-treatment, H&E staining revealed reduced solar elastosis and a threefold increase in Grenz zone papillary collagen. A significant increase in fibrillary tissue was observed, with a more organized fascicular pattern composed of young, thicker, and shorter fibers (Figure 5). Masson's Trichrome staining (Figure 6) similarly showed a pronounced increase in papillary collagen with younger, thicker, and less wavy fibers. Elastin content

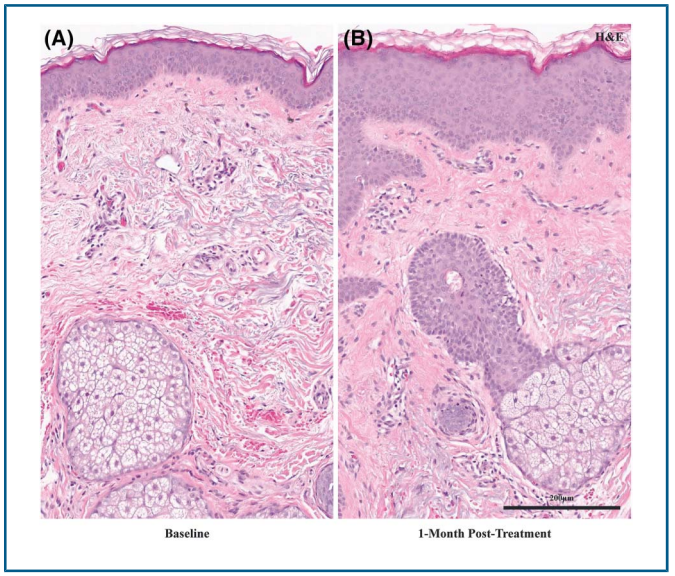

Figure 2. H&E staining at 1-month post-treatment. Representative submental skin biopsies from a 63-year-old woman with Fitzpatrick skin type III. Pretreatment (A) and 1-month post-treatment (B) images show the epidermal and dermal layers. Collagen fibers within the dermis appear light pink. Scale bar: 200 μm.

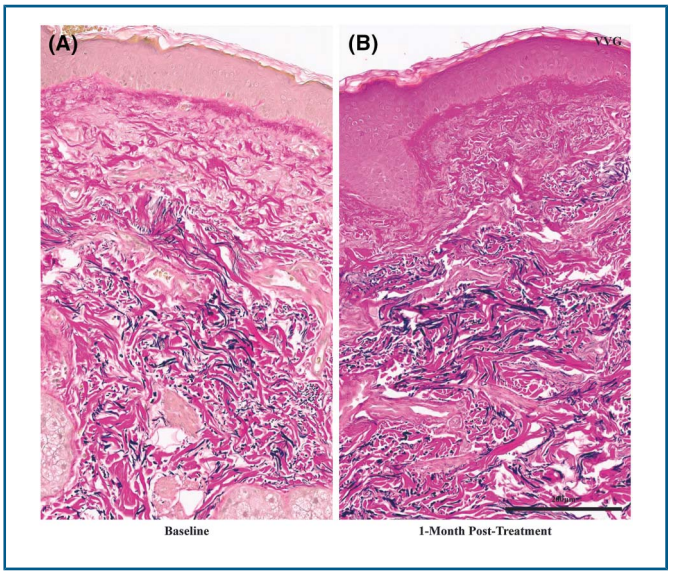

Figure 4. VVG staining at 1-month post-treatment. Representative submental skin biopsies from a 50-year-old woman with Fitzpatrick skin type I. Pretreatment (A) and 1-month post-treatment (B) images show the epidermal and dermal layers. Collagen fibers appear pink, while elastic fibers are stained black. Scale bar: 200 μm. VVG, Verhoeff–Van Gieson.

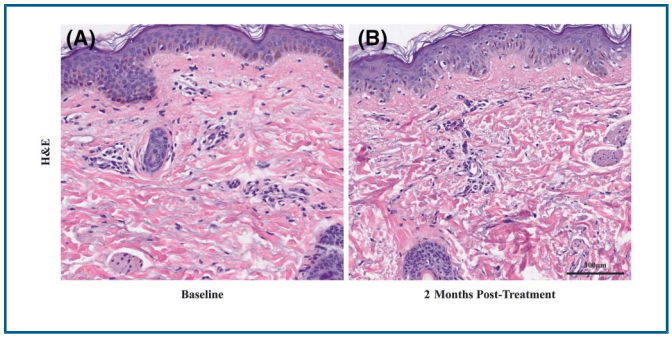

Figure 5. H&E staining at 2-month post-treatment. Representative submental skin biopsies from a 76-year-old woman with Fitzpatrick skin type V. Pretreatment (A) and 2-month post-treatment (B) images show the epidermal and dermal layers. Collagen fibers within the dermis appear light pink. Scale bar: 100 μm.

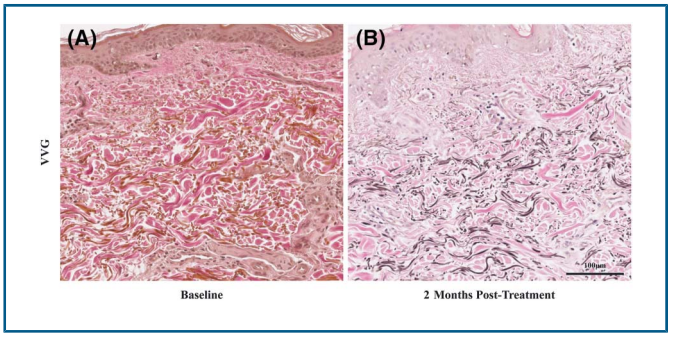

Figure 7. VVG staining at 2-month post-treatment. Representative submental skin biopsies from a 77-year-old woman with Fitzpatrick skin type V. Pretreatment (A) and 2-month post-treatment (B) images show the epidermal and dermal layers. Collagen fibers appear light pink, while elastic fibers are stained black. Scale bar: 100 μm. VVG, Verhoeff–Van Gieson.

increased significantly throughout the dermis, with visibly thicker fibers (Figure 7).

At 4 months post-treatment, Unna Taenzer staining (Figure 8) showed enhanced elastin fiber density across all dermal layers, with the highest concentration at the papillary dermis and upper reticular dermis. The elastin morphology shifted from amorphous to a highly organized configuration. Collagen fibers also showed a significant increase, particularly in the papillary dermis.

At 7 months post-treatment, the dermis exhibited a notable improvement in structural organization, with collagen fibers aligned in parallel manner to the epidermis (Figure 9A). Unna Taenzer staining showed increased collagen and elastin content across all dermal layers, with elastin transitioning from amorphous at baseline to a more structured and highly organized configuration (Figure 9B). Collagen intensification was greatest in the lower dermis. Alcian Blue staining (Figure 9C), used to visualize GAGs including HA, revealed significantly denser light blue staining at 7 months post-treatment. This indicates a substantial increase in HA content, improved fiber alignment, and overall dermal thickening.

At 10 months post treatment, H&E staining demonstrated a sustained and significant increase in dermal collagen density (Figure 10A). The increase in both collagen and elastin throughout the dermis was accompanied by a clear morphological shift to a highly organized, parallel fiber arrangement, along with a marked increase in HA content (Figure 10B,C).

Discussion

Synchronous Parallel Ultrasound technology successfully induced ECM remodeling in both the papillary and reticular dermis. Collagen synthesis during the wound healing process begins within the first few days postinjury, during the late inflammatory phase, peaks around 1-month post-injury, during the transition from the proliferative to the early remodeling phase and continues throughout the later proliferation and remodeling phases.[8,27,28] Unlike collagen, elastin does not exhibit a sharp production peak but continues to be synthesized at lower, sustained levels throughout the remodeling phase.[29,30] Consistent with these reports, the authors observed a significant increase in connective tissue collagen and elastin at 1-month post-

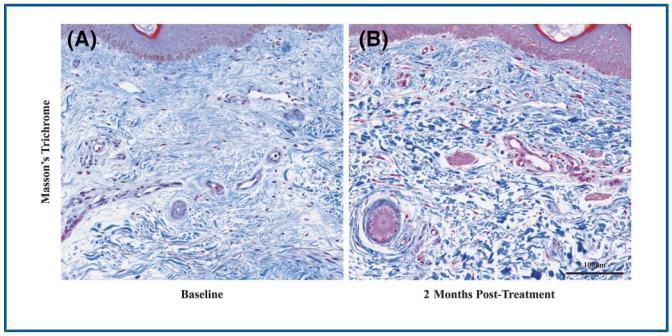

Figure 6. Masson's Trichrome staining at 2-month post-treatment. Representative submental skin biopsies from a 63-year-old woman with Fitzpatrick skin type IV. Pretreatment (A) and 2-month post-treatment (B) images show the epidermal and dermal layers. Collagen fibers within the dermis appear blue. Scale bar: 100 μm.

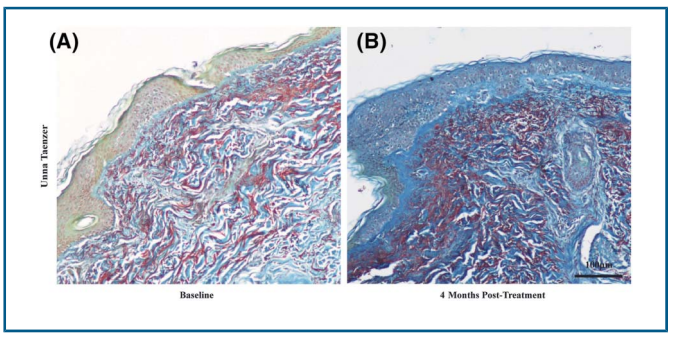

Figure 8. Unna Taenzer staining at 4-month post-treatment. Representative submental skin biopsies from a 40-year-old woman with Fitzpatrick skin type III. Pretreatment (A) and 4-month post-treatment (B) images show the epidermal and dermal layers. Collagen fibers appear blue, while elastic fibers are stained red. Scale bar: 100 μm.

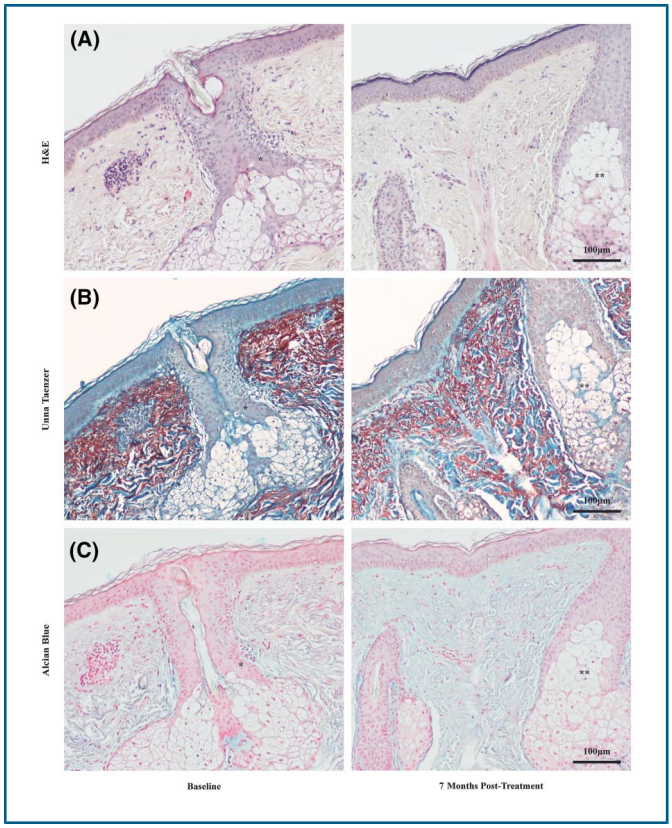

Figure 9. Histochemical staining at 7-month post-treatment. Representative submental skin biopsies from a 48-year-old woman with Fitzpatrick skin type IV. Biopsy specimens stained with H&E (A) Unna Taenzer (B), and Alcian Blue (C). Collagen stained in light pink (A) and blue (B) within the dermis. Elastic fibers are stained in red (B). Glycosaminoglycans are stained in blue (C) within the dermis. Pretreatment and post-treatment images are indicated in the figure. Landmarks of consecutive sections are depicted in the figure, *in pretreatment, and **in post-treatment. Scale bar: 100 μm. GAGs, Glycosaminoglycans.

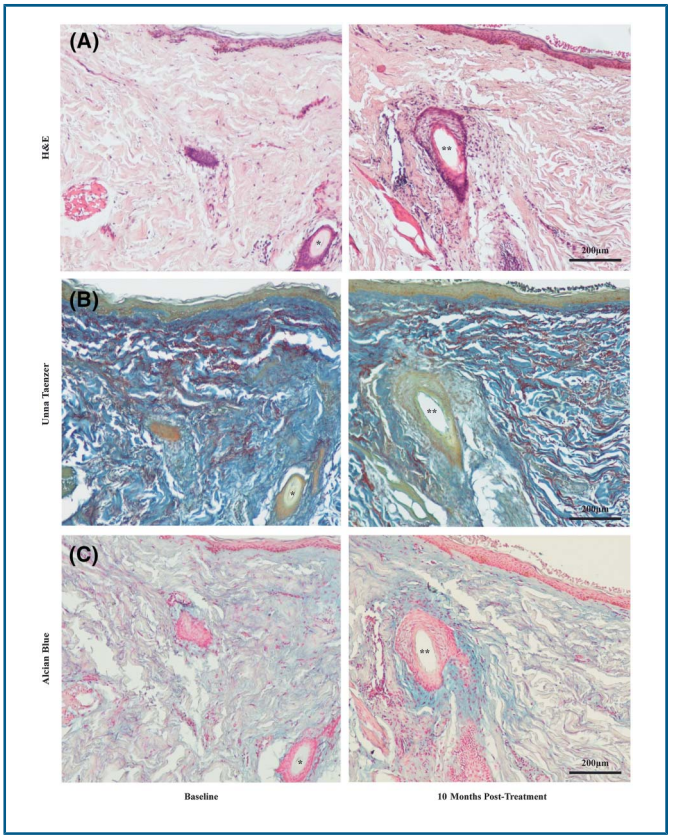

Figure 10. Histochemical staining at 10-month post-treatment. Representative submental skin biopsies from a 60-year-old woman with Fitzpatrick skin type III. Biopsy specimens stained with H&E (A) Unna Taenzer (B), and Alcian Blue (C). Collagen stained in light pink (A) and blue (B) within the dermis. Elastic fibers are stained in red (B). Glycosaminoglycans are stained in blue (C) within the dermis. Pretreatment and post-treatment images are indicated in the figure. Landmarks of consecutive sections are depicted in the figure, *in pretreatment, and **in post-treatment. Scale bar: 200 μm. GAGs, Glycosaminoglycans.

treatment, along with unique reorganization and parallel realignment of dermal fibers.

Extracellular matrix remodeling induced by Synchronous Parallel Ultrasound followed the expected wound healing stages. At 2 months post-treatment, the authors observed a reduction in solar elastosis and a significant threefold increase in Grenz zone papillary collagen, along with a significant increase in fibrillary tissue. The newly formed collagen fibers and bundles showed fascicular patterns with thick, short morphology. Elastin content was also significantly increased, accompanied by a more organized structure and thicker fiber appearance across the dermis. These findings align with the report by Suh and colleagues,[17] who demonstrated well-organized, tightly packed fibers and increased dermal collagen and elastic fiber density 2 months after Synchronous Parallel Ultrasound treatment.

The literature describes the remodeling and maturation phases of wound healing as prolonged processes, continuing for several months postinjury. In conformity, their 4-month post-treatment results showed increased collagen and elastin densities across the dermal layer and particularly in the papillary dermis and upper reticular dermis, along with a highly organized fiber configuration. By 10 months post-treatment, the authors observed sustained tissue remodeling marked by enhanced GAG production and improved ECM alignment and organization. These observations support the notion of ongoing ECM regeneration well-beyond the acute wound healing phase, with continued production of collagen, elastin, and GAGs.[28,31,32]

As previously discussed, wound healing is a complex biological process involving numerous signaling molecules. Various cytokines and GFs such as transforming growth factor-beta (TGFβ), TGFα, fibroblast growth factor, hepatocyte growth factor, and insulin-like GF-1 (IGF-1) are typically released within the first few hours to days after cutaneous injury, driving the dynamic regenerative processes.[33–39] Transforming growth factor-beta is a major regulator of protein synthesis in human skin, contributing to tissue homeostasis and playing a key role in wound healing by modulating reepithelialization and granulation tissue formation through both Smad-dependent and Smad-

independent pathways.[33] Cell responses to collagen are mediated through integrin receptors on cell surfaces. Integrin activation by collagen is also responsible for activating signal transduction pathways controlling matrix remodeling. Furthermore, it has been shown that denatured collagen stimulates a more rapid and robust remodeling into new ECM.[12] The authors hypothesized that integrin binding of RGD sites that became exposed on denatured collagen molecules post-treatment triggered the observed strong neocollagenesis and neoelastogenesis.[12] Furthermore, the authors believe that their histological findings could help guide clinical recommendations regarding the optimal window to perform a maintenance treatment. Their data at 1- and 2-month post-treatment support boosting the healing response with a second treatment at the time of transitioning from the late proliferative into the remodeling phase. This study included 11 patients, as an outlook, the authors would suggest increasing the sample size for more precise and comprehensive statistical analysis. Moreover, incorporating molecular biomarkers associated with different stages of wound healing could further elucidate the biological mechanisms underlying the observed clinical outcomes. Specifically, evaluating the expression patterns of cytokines and remodeling enzymes such as TGFβ, MMP-1, MMP-3, and MMP-9 during the late remodeling phase may further provide insights into long-term tissue regeneration. Future investigations should include multiple time points across all wound healing phases to capture the dynamic nature of ECM regeneration.

Their results provide histological evidence of long-term dermal ECM remodeling induced by Synchronous Parallel Ultrasound and establish strong groundwork for future research into the physiological mechanisms underlying the skin regenerative effects of Synchronous Parallel Ultrasound.

References

1. Nyström A, Bruckner-Tuderman L. Matrix molecules and skin biology. *Semin Cell Dev Biol* 2019;89:136–46.
2. Smith LT, Holbrook KA, Madri JA. Collagen types I, III, and V in human embryonic and fetal skin. *Am J Anat* 1986;175:507–21.
3. Baumann L, Bernstein EF, Weiss AS, Bates D, et al. Clinical relevance of elastin in the structure and function of skin. *Aesthet Surg J Open Forum* 2021;3:ojab019.
4. Varani J, Dame MK, Rittie L, Fligiel SE, et al. Decreased collagen production in chronologically aged skin: roles of age-dependent alteration in fibroblast function and defective mechanical stimulation. *Am J Pathol* 2006;168:1861–8.
5. Dumas M, Chaudagne C, Bonté F, Meybeck A. In vitro biosynthesis of type I and III collagens by human dermal fibroblasts from donors of increasing age. *Mech Ageing Dev* 1994;73:179–87.
6. Maisel A, Waldman A, Furlan K, Weil A, et al. Self-reported patient motivations for seeking cosmetic procedures. *JAMA Dermatol* 2018; 154:1167–74.
7. Thomason HA, Hardman MJ. Delayed wound healing in elderly people. *Rev Clin Gerontol* 2009;19:171–84.
8. Broughton G 2nd, Janis JE, Attinger CE. The basic science of wound healing. *Plast Reconstr Surg* 2006;117:12S–34S.
9. Yarmolenko PS, Moon EJ, Landon C, Manzoor A, et al. Thresholds for thermal damage to normal tissues: an update. *Int J Hyperthermia* 2011;27:320–43.
10. Dams SD, de Liefde-van Beest M, Nuijs AM, Oomens CW, et al. Pulsed heat shocks enhance procollagen type I and procollagen type III expression in human dermal fibroblasts. *Skin Res Technol* 2010;16:354–64.
11. Dams SD, de Liefde-van Beest M, Nuijs AM, Oomens CW, et al. Heat shocks enhance procollagen type I and III expression in fibroblasts in ex vivo human skin. *Skin Res Technol* 2011;17:167–80.
12. Abraham LC, Dice JF, Lee K, Kaplan DL. Phagocytosis and remodeling of collagen matrices. *Exp Cell Res* 2007;313:1045–55.
13. Díaz SH, Nelson JS, Wong BJ. Rate process analysis of thermal damage in cartilage. *Phys Med Biol* 2003;48:19–29.
14. Bozec L, Odlyha M. Thermal denaturation studies of collagen by microthermal analysis and atomic force microscopy. *Biophys J* 2011; 101:228–36.
15. Hovhannisyan VA, Su PJ, Lin SJ, Dong CY. Quantifying thermodynamics of collagen thermal denaturation by second harmonic generation imaging. *Appl Phys Lett* 2009;94.
16. Jia X, Feng Y. Energy-based skin rejuvenation: a review of mechanisms and thermal effects. *J Cosmet Dermatol* 2025;24:e16657.
17. Suh DH, Lee SJ, Song KY, Ahn HJ, et al. High-intensity, parallel ultrasound tightening of facial skin: clinical and pathologic results. *J Cosmet Dermatol* 2025;24:e16670.
18. Wang JV, Ferzli G, Jeon H, Geronemus RG, et al. Efficacy and safety of high-intensity, high-frequency, parallel ultrasound beams for fine lines and wrinkles. *Dermatol Surg* 2021;47:1585–9.
19. Hongcharu W, Boonchoo K, Gold MH. The efficacy and safety of the high-intensity parallel beam ultrasound device at the depth of 1.5 mm for skin tightening. *J Cosmet Dermatol* 2023;22:1488–94.
20. Wang JV, Ugonabo N, Bajaj S, Jairath N, et al. High-intensity, high-frequency, parallel ultrasound beams for cellulite of the buttocks and thighs. *Dermatol Surg* 2024;50:922–5.
21. Gold MH, Biron J. Efficacy and safety of high-intensity, high-frequency, non-focused ultrasound parallel beams for facial skin laxity. *J Cosmet Dermatol* 2024;23:117–23.
22. Boonchoo K, Hongcharu W. The efficacy and safety of a single treatment of high-intensity, high-frequency, non-focused ultrasound parallel beams for facial acne scars in Asian patients: a preliminary study. *J Cosmet Dermatol* 2025;24:e70134.
23. Wang JV, Bajaj S, Geronemus RG, Kauvar A. High-intensity, high-frequency, parallel ultrasound beams for submental lifting. *Dermatol Surg* 2023;49:532–4.
24. Wang JV, Bajaj S, Kauvar A, Geronemus RG. Eyebrow lifting from high-intensity, high-frequency, parallel ultrasound beams. *Dermatol Surg* 2023;49:718–20.
25. Wong A, Lowery AS, Bloom JD. Ultrasound therapy for the skin. *Facial Plast Surg Clin North Am* 2023;31:503–10.
26. Oku K. Vectorized facial skin tightening: a study on the thermal thread technique™ utilizing high-intensity, high-frequency, parallel ultrasound beam. *Lasers Surg Med* 2024;56:355–60.
27. Landén NX, Li D, Ståhle M. Transition from inflammation to proliferation: a critical step during wound healing. *Cell Mol Life Sci* 2016; 73:3861–85.
28. Rittié L. Cellular mechanisms of skin repair in humans and other mammals. *J Cell Commun Signal* 2016;10:103–20.
29. Ashcroft GS, Kielty CM, Horan MA, Ferguson MW. Age-related changes in the temporal and spatial distributions of fibrillin and elastin mRNAs and proteins in acute cutaneous wounds of healthy humans. *J Pathol* 1997;183:80–9.
30. Tracy LE, Minasian RA, Caterson EJ. Extracellular matrix and dermal fibroblast function in the healing wound. *Adv Wound Care (New Rochelle)* 2016;5:119–36.
31. Singh D, Rai V, Agrawal DK. Regulation of collagen I and collagen III in tissue injury and regeneration. *Cardiol Cardiovasc Med* 2023;7:5–16.
32. Talbott HE, Mascharak S, Griffin M, Wan DC, et al. Wound healing, fibroblast heterogeneity, and fibrosis. *Cell Stem Cell* 2022;29:1161–80.
33. Ramirez H, Patel SB, Pastar I. The role of TGFβ signaling in wound epithelialization. *Adv Wound Care (New Rochelle)* 2014;3:482–91.
34. Fabi S, Sundaram H. The potential of topical and injectable growth factors and cytokines for skin rejuvenation. *Facial Plast Surg* 2014;30: 157–71.

35. Costantini E, Aielli L, Serra F, De Dominicis L, et al. Evaluation of cell migration and cytokines expression changes under the radiofrequency electromagnetic field on wound healing in vitro model. *Int J Mol Sci* 2022;23:2205.
36. Peplow PV, Chatterjee MP. A review of the influence of growth factors and cytokines in in vitro human keratinocyte migration. *Cytokine* 2013;62:1–21.
37. Liarte S, Bernabé-García Á, Nicolás FJ. Role of TGF-β in skin chronic wounds: a keratinocyte perspective. *Cells* 2020;9:306.
38. Hantash BM, Zhao L, Knowles JA, Lorenz HP. Adult and fetal wound healing. *Front Biosci* 2008;13:51–61.
39. Li Y, Fan J, Chen M, Li W, et al. Transforming growth factor-alpha: a major human serum factor that promotes human keratinocyte migration. *J Invest Dermatol* 2006;126:2096–105.